New insights into cytotoxic mechanisms of bozepinib against glioblastoma

Amanda de Fraga Dias [a], Juliete Nathali Scholl [a], Cesar Eduardo Jacintho Moritz [b],
Luciano Porto Kagami [c], Gustavo Machado das Neves [c], Vera Lúcia Eifler-Lima [c],
Olga Cruz-López [d,e], Ana Conejo-García [d,e], Jean Sévigny [f,g], Ana Maria Oliveira Battastini [a,h],
Joaquin María Campos [d,e], Fabrício Figueiró [a,h,*]

[a] Programa de Pós-Graduação em Ciências Biológicas: Bioquímica, Instituto de Ciências Básicas da Saúde, Universidade Federal do Rio Grande do Sul, Porto Alegre, RS, Brazil

[b] Programa de Pós-Graduação em Ciências do Movimento Humano, Escola de Educação Física, Fisioterapia e Dança, Universidade Federal do Rio Grande do Sul, Porto Alegre, RS, Brazil

[c] Laboratório de Síntese Orgânica Medicinal/LaSOM, Programa de Pós-Graduação em Ciências Farmacêuticas/PPGCF, Faculdade de Farmácia, Universidade Federal do Rio Grande do Sul, Porto Alegre, RS, Brazil

[d] Departamento de Química Farmacéutica y Orgánica, Facultad de Farmacia, Campus de Cartuja, Granada, Spain

[e] Instituto de Investigacion Biosanitaria ibs.GRANADA, Granada, Spain.

[f] Département de Microbiologie-Infectiologie et d'Immunologie, Faculté de Médecine, Université Laval, QC, Québec, Canada.

[g] Centre de recherche du CHU de Québec – Université Laval, Québec city, QC G1V 4G2, Canada.

[h] Departamento de Bioquímica, Instituto de Ciências Básicas da Saúde, Universidade Federal do Rio Grande do Sul, Porto Alegre, RS, Brazil

ARTICLE INFO

ABSTRACT

Glioblastoma (GBM) is the most frequent and aggressive brain tumor in adults and the current treatments only have a modest effect on patient survival. Recent studies show that bozepinib (BZP), a purine derivative, has potential applications in cancer treatment. The aim of this study was to evaluate the effect of BZP against GBM cells, specially concerning the purinergic system. Thus, GBM cells (C6 and U138 cell lines) were treated with BZP and cell viability, cell cycle, and annexin/PI assays, and active caspase-3 measurements were carried out. Besides, the effect of BZP over the purinergic system was also evaluated *in silico* and *in vitro*. Finally, we evaluate the action of BZP against important markers related to cancer progression, such as Akt, NF-κB, and CD133. We demonstrate here that BZP reduces GBM cell viability ($IC_{50} = 5.7 \pm 0.3$ μM and 12.7 ± 1.5 μM, in C6 and U138 cells, respectively), inducing cell death through caspase-dependent apoptosis, autophagosome formation, activation of NF-κB, without any change in cell cycle progression or on the Akt pathway. Also, BZP modulates the purinergic system, inducing an increase in CD39 enzyme expression and activity, while inhibiting CD73 activity and adenosine formation, without altering CD73 enzyme expression. Curiously, one cycle of treatment resulted in enrichment of GBM cells expressing NF-κB and CD133$^+$, suggesting resistant cells selection. However, after another treatment round, the resistant cells were eliminated. Altogether, BZP presented *in vitro* anti-glioma activity, encouraging further *in vivo* studies in order to better understand its mechanism of action.

1. Introduction

Gliomas are the most frequent brain tumors in adults, accounting for about 26% of all primary brain and other central nervous system (CNS) tumors and 81% of malignant tumors in the United States (Ostrom et al., 2019). More than half of diagnosed gliomas are glioblastomas (GBMs); accounted for 14.6% of all primary CNS tumors and 48.3% of primary malignant brain tumors (Barnholtz-Sloan et al., 2018; Ostrom et al.,

2019). Current standard therapy for GBM, referred to as the 'Stupp protocol' (Stupp et al., 2005; Mutter and Stupp, 2006), includes maximal safe surgical resection followed by radio- and chemotherapy, the latter with the alkylating agent Temozolomide (TMZ, Temodal®). Although TMZ chemotherapy improves the median survival of patients from 12.1 to 14.6 months (Zhu et al., 2017; Herbener et al., 2020; Yan et al., 2020), 90% of recurrent GBM are insensitive to repetitive TMZ treatment due to tumor-developed chemoresistance (Wijaya et al., 2017;
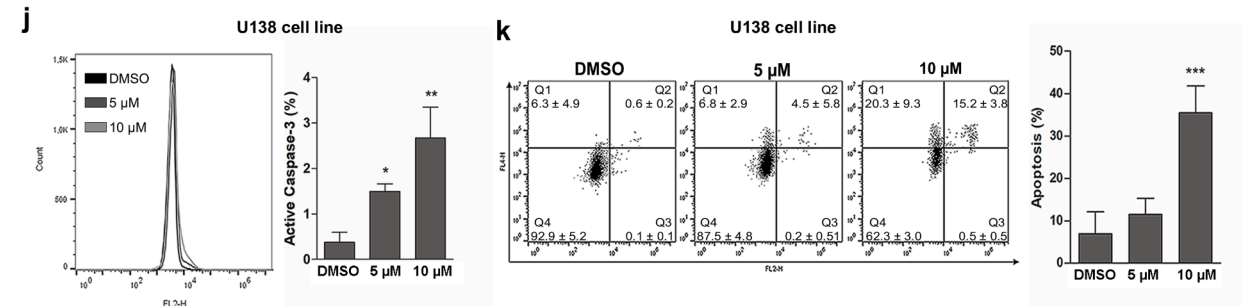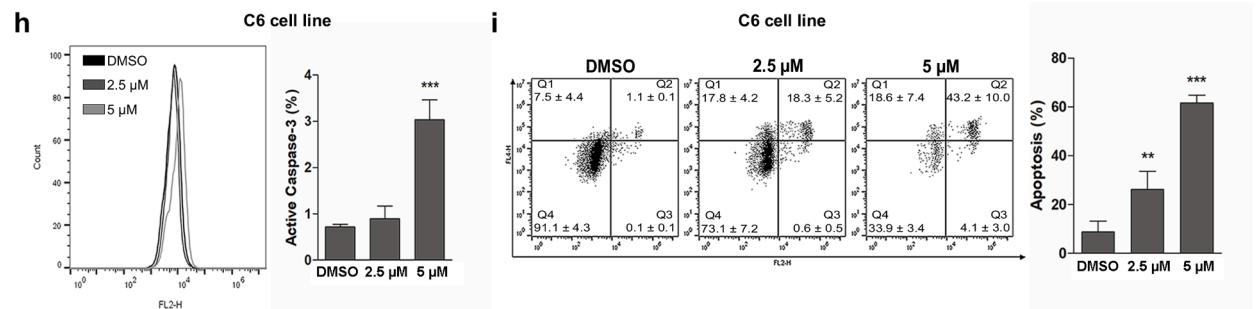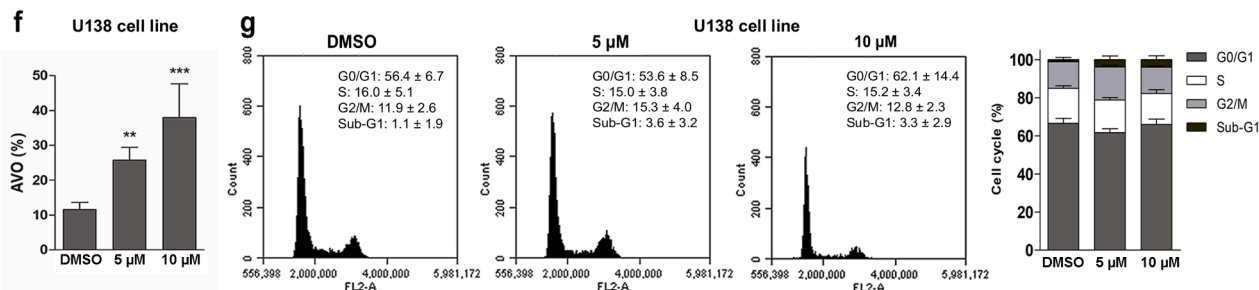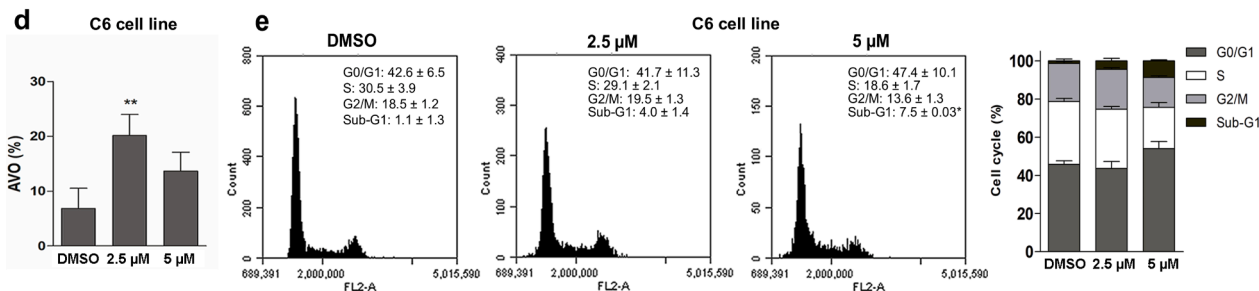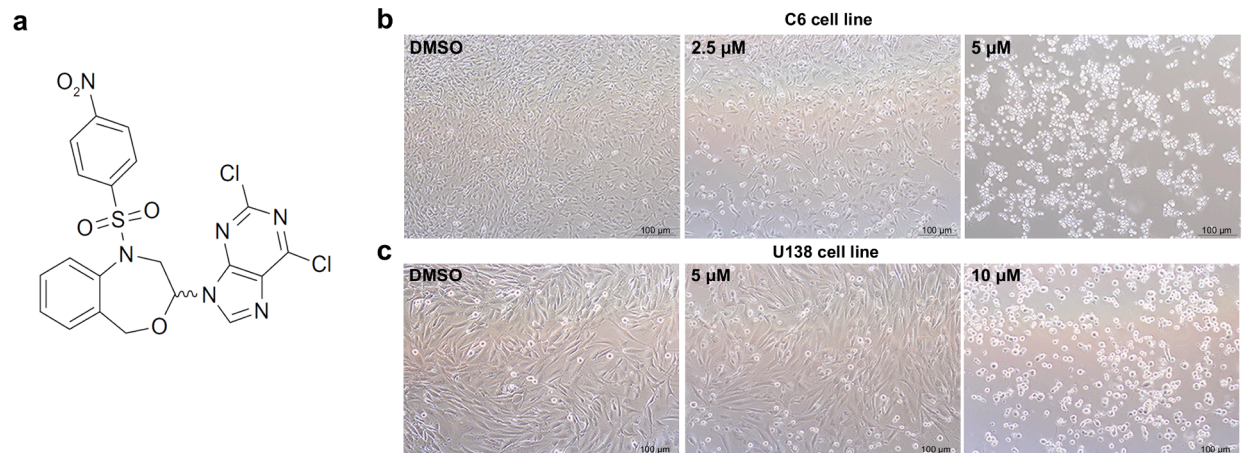
(caption on next page)

Fig. 1. BZP induces cell death by apoptosis, with activation of caspase-3 and formation of AVO, without interference in the cell cycle progression. GBM cells were treated with BZP (2.5 μM/5 μM for C6 cell lines and 5 μM/10 μM for U138 cell lines) for 24 h. (a) BZP (b) Images of C6 cells under microscope (scale bar, 100 μm; magnification, ×100). (c) Images of U138 cells under microscope (scale bar, 100 μm; magnification, ×100). (d) AVO, represented as % of cells in C6 cells. (e) Histogram and quantitative cell cycle analysis in C6 cells. (f) AVO, represented as % of cells in U138 cells. (g) Histogram and quantitative cell cycle analysis in U138 cells. (h) Histogram and quantitative Active Caspase-3 immunocontent analysis in C6 cells. (i) Dot-plot (Q1 = early apoptosis, Q2 = late apoptosis, Q3 = necrosis and Q4 = viable cells) and quantitative analysis of apoptosis in C6 cells. (j) Histogram and quantitative Active Caspase-3 immunocontent analysis in U138 cells. (k) Dot-plot (Q1 = early apoptosis, Q2 = late apoptosis, Q3 = necrosis and Q4 = viable cells) and quantitative analysis of apoptosis in U138 cells. Data are presented as mean ± S.D. of three independent experiments. (*p<0.05 **p<0.01 *** p<0.001).

Azambuja et al, 2020). Considering this scenario, the development of new therapeutic strategies and related drugs is urgently needed to substantially improve the prognosis of GBM patients.

Bozepinib (BZP), (*RS*)-2,6-dichloro-9-[1-(*p*-nitrobenzenesulfonyl)-1,2,3,5-tetrahydro -4,1-benzoxazepin-3-yl]-9*H*-purine (Fig. 1a), is a potent research compound for the treatment of cancer. BZP induces cell death *in vitro* by apoptosis by modulating the PKR protein kinase, which has been shown to be its biological target and involved in the apoptosis of breast and colon cancer cells (Marchal et al., 2013). In addition, BZP is also able to specifically inhibit HER2, JNK and ERKs, while induces the downregulation of genes involved in the formation of cancer stem cells (CSCs), cells responsible for metastasis and tumor resistance to conventional therapies (Ramírez et al., 2014). The CSCs play an important role in the development of chemo and radiotherapy resistance and are primarily responsible for GBM recurrence after initial therapy. Hence new therapeutic approaches that are effective in eliminating glioma stem cells (GSCs) are urgently needed (Yamada and Nakano, 2012; Uribe et al., 2017). *In vivo,* BZP showed interesting antiproliferative results in breast cancer without presenting detectable toxicity to the liver, kidneys or systemic damage. (Ramírez et al., 2014). The antitumor and antimetastatic effect and the non-systemic toxicity of BZP described in the work of Ramírez et al. (2014), encouraged further studies on the therapeutic potential of this novel synthetic compound against cancer. Based on these results, BZP becomes an interesting alternative for research against GBM, since this potential compound may prove to be effective against some resistance mechanisms observed in GBM treated with conventional therapies. In addition, once BZP is derived from a purine, it became an interesting candidate for purinergic system investigation.

The purinergic system is known for its important role in various biological processes (Burnstock and Knight, 2004). Purinergic signaling is composed of ectoenzymes and receptors that are responsible for interaction with extracellular nucleoside and nucleotides derived from purines (Zimmermann, 2001; Burnstock and Knight, 2004; Robson et al., 2006). These extracellular molecules modulate a variety of biological processes via activation of purinergic receptors, controlled by ectonucleotidases, such as E-NTPDase1 (CD39) and ecto-5′-nucleotidase (CD73), which is an integrated way to hydrolyze ATP into adenosine (Zimmermann, 2001; Robson et al., 2006). Several studies have demonstrated the purinergic system is closely involved with the progression of gliomas, both *in vitro* and *in vivo* (Braganhol et al., 2009; Ledur et al., 2012; Allard et al., 2019). It has already been described that GBM, compared to astrocytes, can not efficiently hydrolyze ATP and ADP due to low expression of CD39, while exhibiting high expression of CD73, presenting high AMP hydrolysis, both in human and rat GBM cells (Wink et al., 2003). This results in different stimuli over the purinergic receptors and, consequently, leads to a pro-tumor environment, mainly mediated by adenosine (Wink et al., 2003; Xu et al. 2013; Allard et al., 2019). The aim of this study was to evaluate the effect of BZP against GBM cells, specially concerning the purinergic system.

2. Materials and methods

2.1. Maintenance of cell lines, drugs and treatment

C6 rat glioma cell line, U138 human glioma cell line and MRC-5 human embryonal lung fibroblast cell line were obtained from

American Type Culture Collection (ATCC, USA) and maintained in DMEM, containing 0.5 U/ml penicillin/streptomycin and supplemented with 5% or 10% FBS. Cell lines were kept at 37°C, in a humidified atmosphere of 95% air and 5% CO₂. BZP was dissolved in DMSO and stored at -20°C. For the cell viability assay, cells were seeded in 96-well plates (5×10^3, 7.5×10^3 and 15×10^3 cells/well, for C6, U138, and MRC-5, respectively) and allowed to grow until semi-confluence, GBM cells were treated with 0.1 to 25 μM and MRC-5 cells were treated with 1 to 300 μM of BZP for 24 h, 48 h and 72 h, according to assay. GBM cells were treated with 0.1 to 2000 μM of adenosine 5′-(α,β-methylene) diphosphate (AMPCP), quercetin or BZP for 24 h, 48 h and 72 h. For all other experiments, GBM cells were seeded in 24-well plates (20×10^3 and 30×10^3 cells/well, for C6 and U138, respectively) and grown to semi-confluence. After, the cells were treated with BZP (2.5 and 5 μM for C6 cell lines, and 5 and 10 μM for U138 cells, respectively), for 24 h. The IC$_{25}$ and IC$_{50}$ values were determined by four theoretical equation based on the viability assay. For AMP hydrolysis assay at different times, C6 cells were seeded in 24-well plates (40×10^3, 20×10^3 and 10×10^3) and treated with 1.0 to 100 μM of AMPCP, quercetin or BZP. For the pre-incubation assay, cells were treated with IC$_{50}$ values (AMPCP: 700 μM, quercetin: 500 μM and BZP: 5 μM; AMPCP: 1000 μM, quercetin: 100 μM and BZP: 2.5 μM; AMPCP: 1000 μM, quercetin: 40 μM and BZP: 0.5 μM), for 24 h, 48 h and 72 h, respectively.

2.2. Cell viability assay

After treatment described above, MTS (3-(4,5-dimethylthiazol-2-yl)-5-(3-carboxymethoxy phenyl)-2-(4-sulfophenyl)-2H-tetrazolium) or MTT (3-(4,5-Dimethylthiazol-2-yl)-2,5-diphenyltetrazolium bromide) were performed. For analysis by the MTS method, 20 μL was added directly to each well and incubated for 2h at 37°C and 5% CO₂. After, it was analyzed at 490 nm in a plate reader (Spectramax M5, Molecular Devices, USA). For MTT method, cells were washed twice with PBS and 10 μL MTT diluted in DMEM (5 mg/mL, 100 μL) were added to each well. The cells were incubated for 2h and the absorbance was read at 570-630 nm by plate reader (Spectramax M5, Molecular Devices, USA).

2.3. Cell Cycle, Annexin V-APC/PI and Acridine Orange Staining

For cell cycle analysis, cells were stained with solution containing 0.5mM Tris-HCl (pH 7.6), 3.5mM trisodium citrate, 0.1% NP40 (v/v), 100μg/mL RNAse and 50μg/mL propidium iodide (PI) (10^6 cells/mL). For annexin analysis, cells were suspended in buffer containing Annexin V-APC and PI. For acridine orange (AO) staining, cells were incubated with AO (1μg/mL). At the end of the respective staining, cells were incubated for 15 minutes in the dark and data was collected using flow cytometry (Accuri, BD Biosciences, USA) (Figueiró et al., 2014). The results were analyzed using FlowJo® software (USA).

2.4. Active Caspase-3 immunocontent

We verified active caspase-3 immunocontent according to manufacturer's protocol (PE Active Caspase-3 kit, cat. 550914, BD Biosciences, USA). Briefly, cells were suspended in BD Cytofix/Cytoperm™ solution and incubated for 20min on ice. After, cells were washed with BD Perm/Wash™ buffer (1×) and incubated with active caspase-3 antibody for 30min at room temperature and then analyzed by flow

cytometry (Accuri, BD Biosciences, USA). The results were analyzed using FlowJo® software (USA).

2.5. Molecular docking

The three-dimensional structure of the CD73 enzyme was obtained from Protein Data Bank server and was prepared using Dock Prep module of the Chimera program. The structure chosen for the docking studies was the closed crystalline form III, complexed with AMPCP with resolution of 2.0Å (PDB ID: 4H2I). The water molecules of the model were removed, hydrogens added according to physiological pH and the atomic charges were assigned to the system using AMBER99SB force field. After, the receptor file was saved in MOL2 format. AMPCP and quercetin were obtained through the ChemSpider server (http://www.chemspider.com/) in MOL format. BZP was designed using CORINA Classic server (https://www.mn-am.com/online_demos/corina_demo_interactive) and downloaded in MOL format. Previously, the ligands were prepared using the Open Babel package (http://openbabel.org). Hydrogens were added according to pH 7.4 and minimized using the Obminimize module with the MMFF94 force field and 2500 steps. The ligands atomic charges were assigned using AM1-BCC charge method. AMPCP's charge was assigned to -2. BZP's and quercetin's charges were assigned to 0. The ligands were converted to MOL2 format. For the molecular docking DOCK 6.7 program and its modules were used (Kuntz et al., 1982; Ferrin, et al., 1988; Meng et al., 1992; Shoichet et al., 1992; Ewing et al., 2001). Two scoring functions were used for molecular coupling studies: Grid Score and Hawkins GB/SA (MM-GB/SA). Analyses of the root-mean-square deviations (RMSD) with respect to reference structures, in a redocking routine, were carried out with fconv (Neudert and Klebe, 2011). For the study of the receptor-ligand interactions, we evaluated the connections between the binding site of CD73 and the predicted best pose of the docked compounds. It is understood as pose, the ensemble of information related to the position, orientation and conformation adopted by the ligand when influenced by the interaction forces of the amino acid residues. For this study the Receiver-Ligand Interactions module of the Discovery Studio 2017 R2-BIOVIA® program was used.

2.6. CD39 and CD73 immunocontent

For the determination of the CD39 and CD73 protein expression, at the end of treatments, cells were washed with 2% FBS, trypsinized and centrifuged twice at $400 \times g$ for 6 min. Next, cells were stained with Polyclonal rabbit anti-rat NTPDase1/CD39 (cat. rN1-6L, J. Sevigny's research lab, CA); APC mouse anti-human CD39 (cat. 560239, BD Biosciences, USA); Polyclonal rabbit anti-rat ecto-5'-Nucleotidase/CD73 (cat. rNu-9L, J. Sevigny's research lab, CA); PE mouse anti-human CD73 (cat. 550257, BD Biosciences, USA) for 30 min on ice and then washed twice. After the last wash, if necessary, the cells were incubated with secondary antibody (Ab) (Alexa Fluor® 633 goat anti-rabbit IgG (cat. A-21070, Invitrogen, USA) for 30 min in the dark and analyzed by flow cytometry (FACSCalibur, BD Biosciences, USA). The results were analyzed using FlowJo® software (USA). A secondary antibody or isotype control was used as a non-specific binding control.

2.7. Purinergic enzymatic assays

2.7.1. Enzymatic assay

In brief, cells were maintained in a water bath at 37°C and washed with incubation medium (2 mM CaCl$_2$ or 2 mM MgCl$_2$, 120 mM NaCl, 5 mM KCl, 10 mM glucose, and 20 mM Hepes buffer, pH 7.4). The enzymatic reaction was initiated by addition of 200 μL of incubation medium containing 1 mM ATP, 1 mM ADP or 2 mM AMP. For the pre-incubation assay, C6 cells were previously treated with 1 to 100 μM of AMPCP, quercetin and BZP for 10 min. Cells were incubated for 10-min (AMP) or 30-min (ATP and ADP) and the reaction was stopped placing 150 μL of

the supernatant in tubes containing ice-cold trichloroacetic acid (5% w/v). The release of inorganic phosphate was measured using malachite green method (Chan et al., 1986). The protein concentration was quantified by Coomassie blue method (Bradford, 1976), using bovine serum albumin as control. The specific activity was expressed in nanomoles of Pi released per minute per milligram of protein.

2.7.2. Recombinant human CD73 assay

Recombinant his-tagged human CD73 (final concentration: 0.005 μg; cat. SRP0570, Sigma-Aldrich, USA) was incubated with 100 μM AMP, in incubation medium (2 mM MgCl$_2$, 120 mM NaCl, 5 mM KCl, 10 mM glucose, and 20 mM Hepes buffer, pH 7.4) and different concentrations of AMPCP, quercetin and BZP (1 to 500 μM) for 25 minutes in 96-well plates. The enzymatic reaction was stopped by addition of 170 μL of malachite green (Chan et al., 1986). The specific activity was expressed as micromoles of Pi released per minute per milligram of protein.

2.7.3. ATP metabolism assay

Cells were maintained in a water bath at 37°C and washed with incubation medium, as previously described. The enzymatic reaction was initiated by addition of 200 μL of incubation medium containing 100 μM ATP. Cells were incubated for 15-, 30- and 45-min and the reaction was stopped by transferring 150 μL of the supernatant to tubes previously placed on ice. Afterwards, the tubes were centrifuged at 16,000 ×g for 30 min at 4°C, and 20 μL aliquots were analyzed by high-pressure liquid chromatography (HPLC) (Shimadzu, Japan) using a C18 column (Gemini C18, 25cm × 4.6mm × 5μm; Phenomenex, USA). The elution was carried out applying a linear gradient from 100% solvent A (60 mM KH$_2$PO$_4$ and 5 mM tetrabutylammonium chloride, pH 6.0) to 100% solvent B (solvent A plus 30 % methanol) for 30 minutes (at a flow rate of 1.4 mL/min) according to a method described previously and already established by our research group (Voelter et al., 1980; Figueiró et al., 2016). The amount of purines was measured by absorption at 254 nm. Purines standards were used to evaluate the retention time of each compound separately allowing the identification and quantification. The protein concentration was quantified with Coomassie blue method, using bovine serum albumin as control. Purine concentrations (AMP and adenosine) are expressed as nanomoles of products per minute per milligram of protein.

2.8. Akt, NF-κB and CD133 immunocontent

In brief, after treatments, cells were washed with PBS, trypsinized and centrifuged twice at $400 \times g$ for 6min with FBS 2%. For Akt and NF-κB immunocontent, cells were incubated with BD Phosflow™ Fix Buffer I for 10min at 37°C. Then, cells were incubated with BD Phosflow™ Perm Buffer III for 30min on ice. Then, for Akt, NF-κB and CD133 immunocontent, cells were stained with PE Mouse anti-Akt (cat. 558275, BD Biosciences, USA), PE Mouse anti-NF-κB p65 (cat. 558423, BD Biosciences, USA), Rabbit polyclonal anti-CD133 (cat. Ab19898, Abcam, USA) plus Alexa Fluor® 633 goat anti-rabbit IgG (cat. A-21070, Invitrogen, USA) antibodies and incubated for 30min in the dark, plus 30 min incubation for specific secondary antibody to primary Ab anti-CD133, and analyzed by flow cytometry (FACSCalibur, BD Biosciences, USA). Results were analyzed using FlowJo® software (USA).

2.9. In vitro recovery assay

After treatment with 5 μM and 10 μM, for C6 and U138, respectively, for 24h, cells were washed with PBS, trypsinized and Trypan Blue dye solution (0.1%) was added. The count of viable cells was immediately performed with a Neubauer chamber. Afterward, the remaining cells were reseeded according to the number of viable cells in the well treated with BZP (limiting value), normalizing control and treatments with the same number of cells. We allowed the growth until semi-confluence and subsequently, the cells were again treated with BZP with the

Table 1
IC_{50} values of BZP in cell lines and *in vitro* SI

Cell lines	IC_{50} (μM) ± SD	SI
C6	5.7 ± 0.3	35
U138	12.7 ± 1.5	15
MRC-5	197.7 ± 9.5 ***	NA

GBM cells were treated with 0.1 to 25 μM of BZP for 24h. MRC-5 cells were treated with 1 to 300 μM of BZP for 24h. Cell viability was determined by MTS assay. SI values were calculated from the IC_{50} value of the MRC-5 / IC_{50} value of GBM cells. Data are means ± S.D. of four independent experiments, *** p< 0.001. SI = selectivity index. NA = not applicable.

abovementioned protocol was repeated until death of the resistant cells.

2.10. Statistical analysis

Data were analyzed for statistical significance by one-way analysis of variance (ANOVA), followed by Tukey post-test using GraphPad Prism software®. Data are expressed as the mean ± S.D. Differences were considered significant when p <0.05.

3. Results and discussion

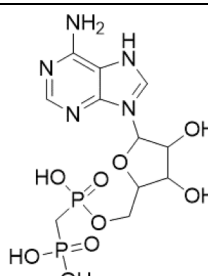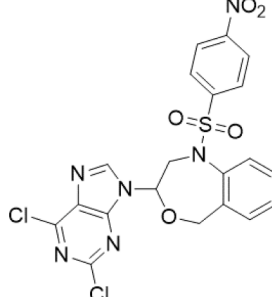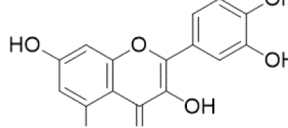### 3.1. BZP reduces cell viability with great selectivity index

Firstly, we determined the effects of BZP in GBM and MRC-5 cells viability to estimate the half-maximum inhibitory concentration (IC_{50}). BZP was able to reduce the percentage of GBM cells with relatively low IC_{50} values (Table 1 and representative pictures of GBM cells after BZP treatment in Figs. 1b and 1c), when compared to other studies that show extremely high IC50 values for TMZ, standard therapy for GBM, with the same cells (~ 500 μM to 1000 μM) (Ryu et al., 2012; Lee, 2016; Li et al., 2017; Towner et al., 2019). In addition, we evaluated the toxicity of BZP for MRC-5 non-tumoral cells, resulting in IC_{50} value 35-fold and 15-fold greater than for C6 and U138, respectively. This shows a selective action of this compound *in vitro*, usually expressed with selectivity index (SI, defined herein as the ratio between IC_{50} of MRC-5 cells / IC_{50} of GBM cells) (Table 1). According to previously published papers, a value greater than or equal to 3.0 is considered an interesting SI (Bézivin et al., 2003; Chothiphirat et al., 2019; Andrade et al., 2020), and values above 10.0 are considered highly selective for cancer cells (Quispe et al., 2006; Peña-Morán et al., 2016).

3.2. BZP induces autophagy and apoptosis without interfering with cell cycle progression

Next, we evaluated the interference of BZP on autophagy, apoptosis, and cell cycle progression. Compounds that induce additional or alternative mechanisms of cell death are very useful in cancer therapy, among them; autophagy is a highly regulated process involved in the degradation of intracellular components by autophagosomes that can be degraded or used to feed metabolic pathways (White et al., 2010; Levy et al., 2017). Thus, we observed that BZP significantly induces the formation of acid vesicle organelles (AVO), as an indication of autophagy (Mizushima et al., 2010; Klionsky et al., 2016; Yang et al., 2020; Lee et al., 2020), at 2.5 μM in C6 cells, about 3-fold greater than the DMSO control (p = 0.0055) (Fig. 1d) and at two concentrations in U138 cells, showing also approximately 3-fold more AVO at the highest concentration tested, compared to the DMSO control (p = 0.0495 and p = 0.0015, for 5 μM and 10 μM, respectively) (Fig. 1f). In cancer, autophagy plays a dichotomous role, being able to suppress tumor growth by cell death or to promote cell growth, contributing to cancer resistance and malignancy (White, 2015; Liu et al., 2017; Onorati et al., 2018). Although it is the target of many studies, the mechanisms underlying these opposite effects, pro or anticancer, induced by autophagy are not

Table 2
Docking results

Structure	Compound	MM-GB/SA (Kcal/mol)	Grid Score (Kcal/mol)
	AMPCP	-119,546	-142,568
	BZP	-52,388	-55,035
	quercetin	-31,24	-43,837

For the molecular docking were used DOCK 6.7 program and two scoring functions were used for molecular coupling studies: A Grid Score and MM-GB/SA.

yet fully elucidated (Levy et al., 2017; Liu et al., 2017; Russo and Russo, 2018; Onorati et al., 2018; Poillet-Peres and White, 2019; Kocaturk et al., 2019).

Therefore, we evaluated the type of cell death induced by BZP treatment staining the cells with Annexin V and PI solution followed by flow cytometry analysis. BZP significantly induced apoptosis in C6 cells (from 9% in DMSO to 36% at 2.5 μM and 62% at 5 μM, p = 0.0090 and p = 0.0001, respectively) (Fig. 1i) and U138 cells also presented significantly higher levels of apoptosis following BZP treatment (from 7% in DMSO to 36% at 10 μM, p = 0.0002) (Fig. 1k). Apoptosis seems to be mediated, at least partially, by active caspase-3 expression in C6 cells and in U138 cells (Figs. 1h and 1j). Drugs that work in apoptotic pathways are promising anti-cancer therapeutic approaches, mainly the ones which selectively induce apoptosis in malignant cells (Wong, 2011; Pistritto et al., 2016; Xu et al., 2019). Thus, results suggest caspase-3-dependent apoptosis is involved in cell death triggered by BZP. Also, BZP treatment does not show any significant change in cell cycle progression, only an accumulation of sub-G1 phase in C6 cells (Figs. 1e and 1g), corroborating apoptosis induction. These results are in agreement with a previously published study with BZP in breast and colon cancer cells (Marchal et al., 2013; Ramírez et al., 2014).

3.3. BZP-CD73 interaction in silico indicates possible enzyme inhibition

Since BZP has a purine in its structure (Fig. 1a), our next step was to investigate the interaction of this compound with the purinergic system. Firstly, we analyzed a possible interaction, *in silico*, of BZP with the CD73 enzyme, widely expressed in glioma cells (Cappellari et al., 2012; Allard et al., 2019; Cerute and Abbrachio, 2020). The docking study (Table 2) showed that BZP interacts energetically with the CD73, as do
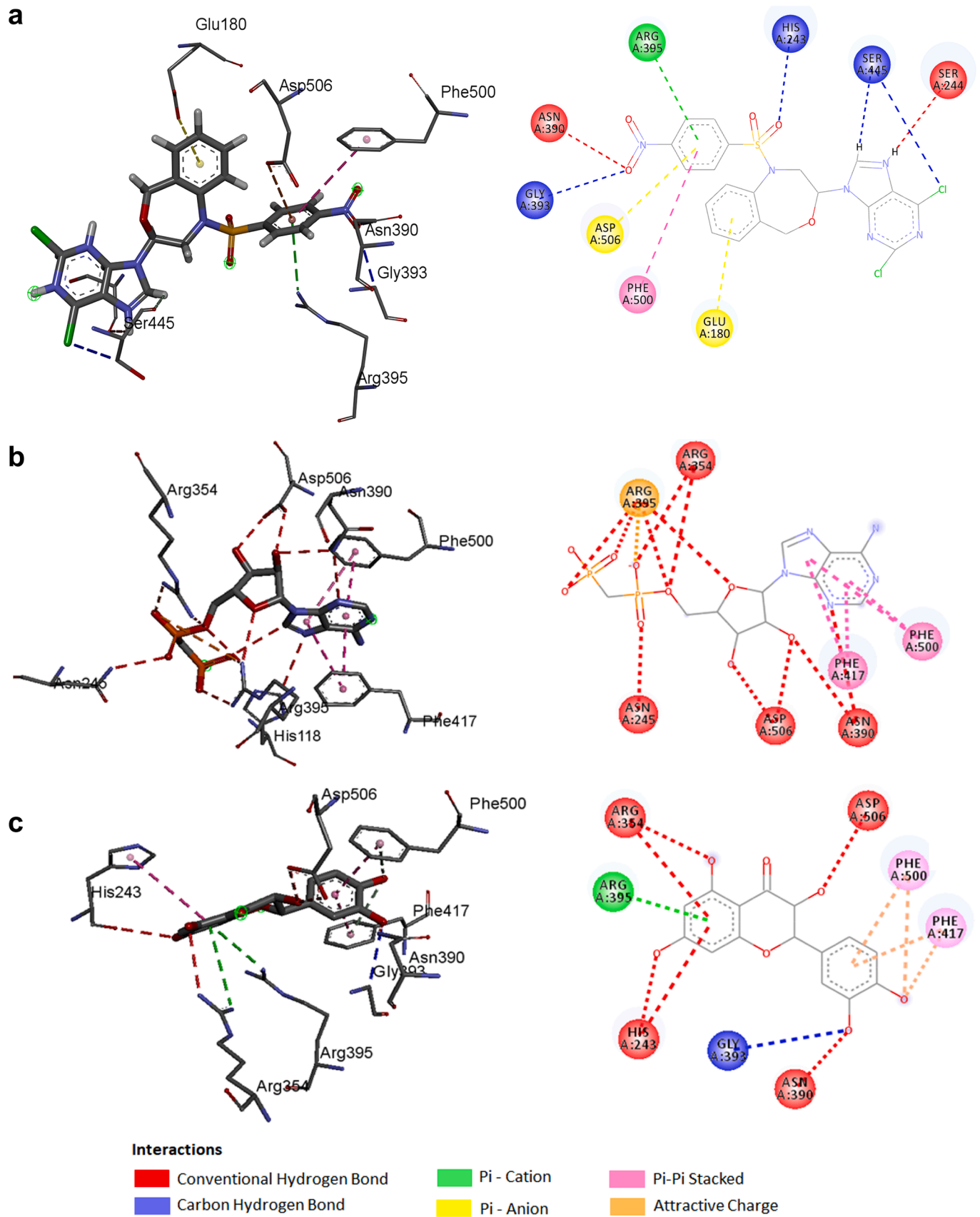
Fig. 2. CD73 and the main interactions with (a) BZP, (b) AMPCP and (c) quercetin.

Table 3

IC_{50} values of AMPCP, quercetin and BZP in cell lines at different treatment times

Compound	IC_{50} (µM) ± SD			
	C6 cells 24h	C6 cells 48h	C6 cells 72h	U138 cells 24h
AMPCP	657.20 ± 69.56	>1000	> 1000	>2000
quercetin	459.29 ± 49.37	95.94 ± 10.74	41.99 ± 13.38	758.21 ± 226.51
BZP	5.61 ± 0.46	2.45 ± 0.20	0.52 ± 0.07	10.06 ± 2.35

GBM cells were treated with 0.1 to 2000 µM of AMPCP, quercetin and BZP for 24h, 48h and 72h. Cell viability was determined by MTT assay. Data are means ± S.D. of four independent experiments.

classical inhibitors of this enzyme, AMPCP and quercetin (Braganhol et al., 2007; Rockenbach et al., 2013; Adamiak et al., 2019; Geraghty et al., 2019). In both MM-GB/SA and Grid scores, BZP showed more favorable interactions to this enzyme than quercetin (2-fold stronger - according to MM-GBSA) and less than AMPCP. Concerning the interaction between receptor-ligand, the Discovery Studio program showed that the major interactions between BZP and CD73 enzyme were Pi-cation interactions with residues Arg395, Pi-anion interactions with residues Asp506 and Glu180, Pi-Pi stacking interactions with Phe500 and conventional hydrogen bond interactions with Asn390 and Ser244 (Fig. 2a). Unlike expected, the BZP purine moiety was not located between Phe417 and Phe500, possibly due to its two coupled chlorine atoms. However, quercetin's dihydroxyphenyl moiety shows a hydrogen bond with Asn390 and Pi-Pi Stacking interactions with Phe417 and Phe500. Other hydrogen interactions occur in the quercetin chromen-4-one moiety with Arg354, Asp506 and His243 residues (Fig. 2c). The interaction of BZP with CD73 is more favorable than quercetin, probably because BZP carries out a hydrogen bond and two more electrostatic interactions than quercetin. In other hand, purine AMPCP portion shows Pi-Pi Stacking interactions with Phe417 and Phe500. There are two hydrogen bonds in the ribose portion with Asp506 and Asn390. In addition, AMPCP phosphate group shows a stronger electrostatic interaction with Arg395 and hydrogen bonds with Arg354 and Asn245 (Fig. 2b). These AMPCP phosphate group electrostatic interactions make the AMPCP-CD73 more favorable than BZP-CD73. The redocking validation showed that the parameters used for the molecular coupling assay were satisfactory (RMSD=2.503Å-excluding hydrogen atoms), since the greatest RMSD value contribution is given by the phosphate-carbon-phosphate moiety (Ramírez and Caballero, 2018).

3.4. BZP differently changes the expression and activity of CD39 and CD73 enzymes

In order to compare the effect of the studied compounds after molecular docking, we evaluated the cell viability in GBM cell lines at different times after treatments with BZP, AMPCP or quercetin. BZP proved to be more effective in reducing cell viability with relatively low IC_{50} values when compared to AMPCP and quercetin, and this was maintained after 24h, 48h and 72h of treatment (Table 3). Some studies have already shown that the inhibitory effect of quercetin in GBM cell lines is dose and time-dependent and closely related to what we described here (Zhou et al., 2006; Braganhol et al., 2006; Kim et al., 2008; Tavana et al., 2020). In addition, we evaluated AMP hydrolysis after treatment with AMPCP, quercetin and BZP. In 24 h only BZP treatment was able to reduce AMP hydrolysis to about 50% (p < 0.001) in C6 cell line (Fig 3a). In 48 h, both AMPCP and BZP reduced the AMP hydrolysis, by approximately 3-fold (p < 0.001) when compared to the control (Fig. 3b). Further, in 72 h, all compounds were able to reduce AMP hydrolysis in C6 cell line, approximately 66% (with 1000 µM), 63% (with 40 µM) and 48% (with 0.5 µM) for AMPCP, quercetin and BZP,

respectively, p < 0.001 (Fig. 3c). Then, we decided to assay the compounds in a short-term experiment. After 10 min of cells' pre-incubation with AMPCP, BZP and quercetin, only AMPCP was able to reduce significantly AMP hydrolysis, showing how fast this classical compound can inhibit the CD73 enzyme (Fig 3d). In U138 cell line, both AMPCP and BZP were able to reduce the AMP hydrolysis within 24 hours after treatment (p < 0.001), approximately 30% and 50%, respectively, (Fig. 3e). When tested in the recombinant CD73, AMPCP inhibits AMP hydrolysis (p < 0.001) at greater extent than quercetin and BZP (Fig. 3f). Quercetin had an intermediate inhibition capability on recombinant CD73 (p < 0.01) significantly inhibiting starting at 10 µM (Fig. 3g). On the other hand, BZP reduced the amount of AMP only at high concentrations (from 250 µM, p < 0.05) when compared to the other compounds (Fig. 3h). Taken together, these results suggest that CD73 inhibition by BZP requires a membrane-anchored enzyme to be effective with lower concentrations than quercetin and AMPCP for 24h, 48h, and 72h (Figs 3a-c and 3e). In contrast, CD73 inhibition by AMPCP is relatively fast and can be effective on purified enzyme and on membrane-anchored enzyme, as demonstrated in the pre-incubation and recombinant CD73 assays (Figs. 3d and 3f). Quercetin, on the other hand, requires a much longer treatment period and higher concentrations to be effective on membrane-anchored enzyme, but, as AMPCP, can inhibit the purified CD73 enzyme (Figs. 3c and 3g).

Afterwards, in view of the encouraging results of BZP in GBM cells, we measured the expression and activity *in vitro* of CD39 and CD73 enzymes. BZP was able to increase approximately 2- and 3-fold the expression of CD39 enzyme in C6 cells and U138 cells, respectively (Figs. 4a and 4b). On the other hand, BZP did not alter the expression of CD73 enzyme in both cell lines under the tested conditions (Figs. 4c and 4d). Measuring the activity, we found that BZP was able to significantly increase the hydrolysis of ATP and ADP in U138 cell line (Fig. 4f), while significantly decreasing the hydrolysis of AMP in both cells by approximately 50% (Figs. 4e and 4f). On the one hand, when we evaluated the metabolism of ATP by HPLC, we found that treatment with BZP increases the amount of extracellular AMP in C6 cells and U138 cells, indicating the functionality of the enzyme CD39. On the other hand, BZP reduced the adenosine formation by inhibiting CD73, approximately 3- and 2-fold in C6 and U138, respectively, in all times tested (Figs. 4g and 4h). BZP treatment did not alter the concentrations of other purine nucleotides and their metabolites when compared to the untreated control (data not shown).

BZP inhibited AMP hydrolysis leading its accumulation, without any change in CD73 expression, indicating a possible direct inhibition of this enzyme. Overall, the modulation of CD39 and CD73 enzymes, caused by BZP treatment, leads to a profile of expression and activity closer to astrocytes since they exhibit high ATPase / ADPase activity and low AMPase activity when compared to GBM cells (Wink et al. 2003). Accordingly, we also found that BZP treatment significantly decreased the formation of adenosine, explaining, at least partially, the cytotoxic effect of BZP in GBM cells. It has been demonstrated that the accumulation of adenosine by the action of CD73 favors tumor growth, metastasis, angiogenesis, chemoresistance, and immunosuppression (Braganhol et al., 2007; Antonioli et al., 2017).

3.5. BZP induces the activation of resistance pathways, however, several treatment cycles are enough to eliminate resistant cells

In cancer development, cells acquire phenotypes of rapid proliferation, invasiveness, malignancy and metastasis formation. Several studies have shown the participation of Akt and NF-κB proteins in cell proliferation and survival, as well as the participation of CD133 in the malignancy and identification of CSCs population in different types of cancer (Soeda et al., 2009; Bai et al., 2009; Yamada et al., 2012; Holmberg et al., 2014; Kim et al., 2017; Brugnoli et al., 2019). In view of this, we evaluated the phosphorylation of Akt, NF-κB and CD133 expressions. Our results showed that BZP did not interfere with Akt
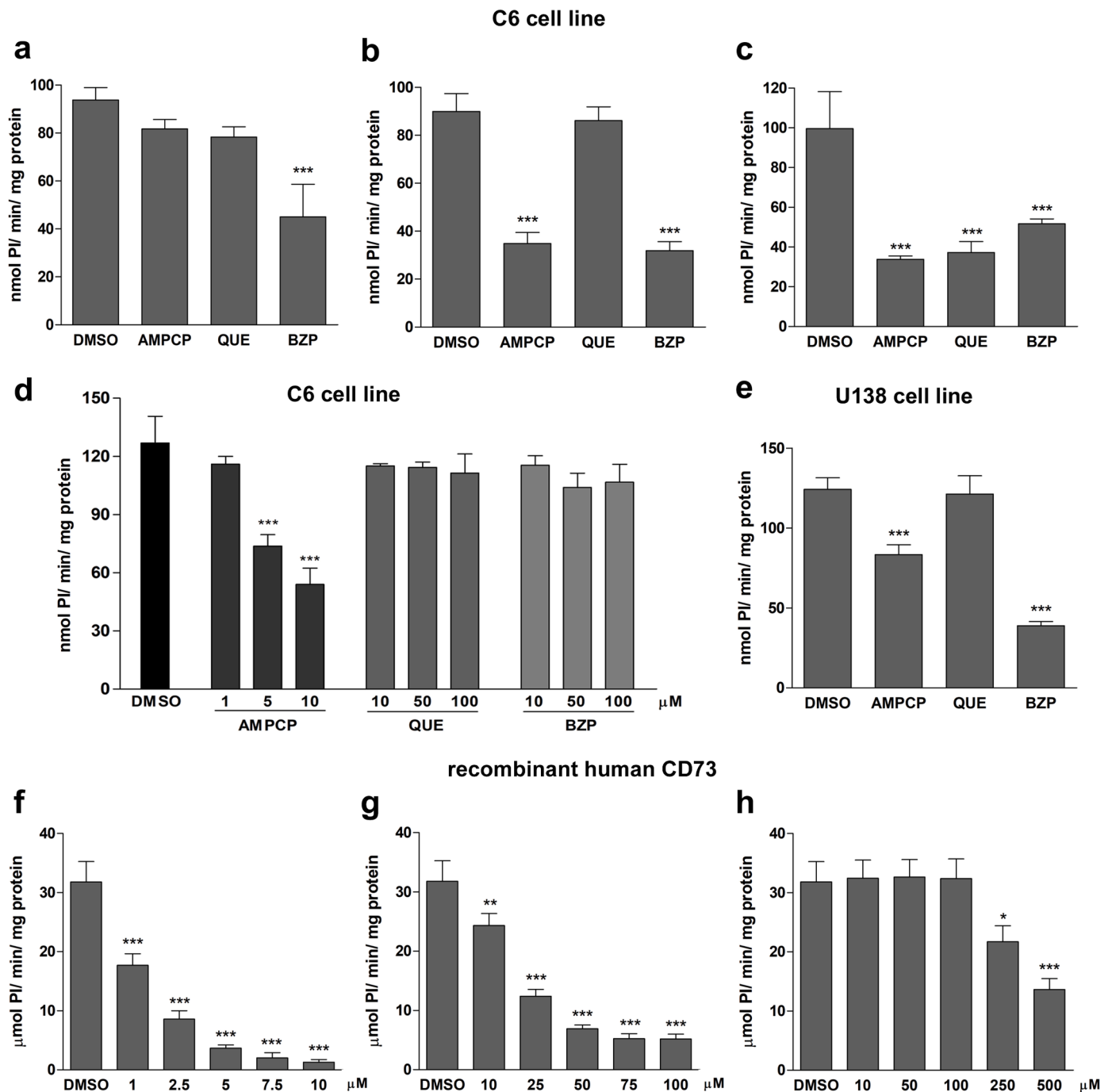
Fig. 3. Effects of AMPCP, quercetin and BZP on AMP hydrolysis in GBM cells and recombinant human CD73 enzyme. (a) AMP hydrolysis in C6 cells treated with AMPCP: 700 μM, quercetin: 500 μM and BZP: 5 μM for 24h. (b) AMP hydrolysis in C6 cells treated with AMPCP: 1000 μM, quercetin: 100 μM and BZP: 2,5 μM for 48h. (c) AMP hydrolysis in C6 cells treated with AMPCP: 1000 μM, quercetin: 40 μM and BZP: 0,5 μM for 72h. (d) AMP hydrolysis in C6 cells pre-incubated for 10 min with AMPCP: 1, 5 and 10 μM, quercetin: 10, 50 and 100 μM and BZP: 10, 50 and 100 μM. (e) AMP hydrolysis in U138 cells treated with AMPCP: 2000 μM, quercetin: 800 μM and BZP: 10 μM for 24h. (f) AMP hydrolysis in recombinant human CD73 enzyme treated with AMPCP: 1 to 10 μM. (g) AMP hydrolysis in recombinant human CD73 enzyme treated with quercetin: 10 to 100 μM. (h) AMP hydrolysis in recombinant human CD73 enzyme treated with BZP: 10 to 500 μM. Data are presented as mean ± S.D. of four (a,b,c,e) or three (d,f,g,h) independent experiments. (*$p<0.05$ **$p<0.01$ *** $p<0.001$). QUE = quercetin.

phosphorylation, when compared to DMSO in both cell lines (Figs. 5a and 5b). However, it was able to increase the phosphorylated p65 NF-κB subunit in C6 cells, p = 0.0017 (Fig. 5c), and in U138 cells, p = 0.0383 (Fig. 5d), indicating an activation of the NF-κB pathway in BZP-resistant cells. Indeed, it is important to note that the protocol, previously described in materials and methods, is quantifying only cells that were still attached to the plate, which are mostly viable cells. The hypothesis here is that the activation of the NF-κB pathway is being a tool for

resistant cells to survive and proliferate even after BZP treatment. The association between NF-κB and CSCs is a target of studies in various types of cancer, and in GBM the phosphorylation of the p65 subunit of NF-κB is elevated in CD133^{+} cells, thus suggesting that NF-κB signaling contributes directly for the maintenance of glioblastoma stem cells (Rinkenbaugh et al., 2016; Kaltschmidt et al., 2019).

Currently, several studies suggest CD133 protein (also known as prominin-1) as a marker of stem cells in normal and cancerous tissues
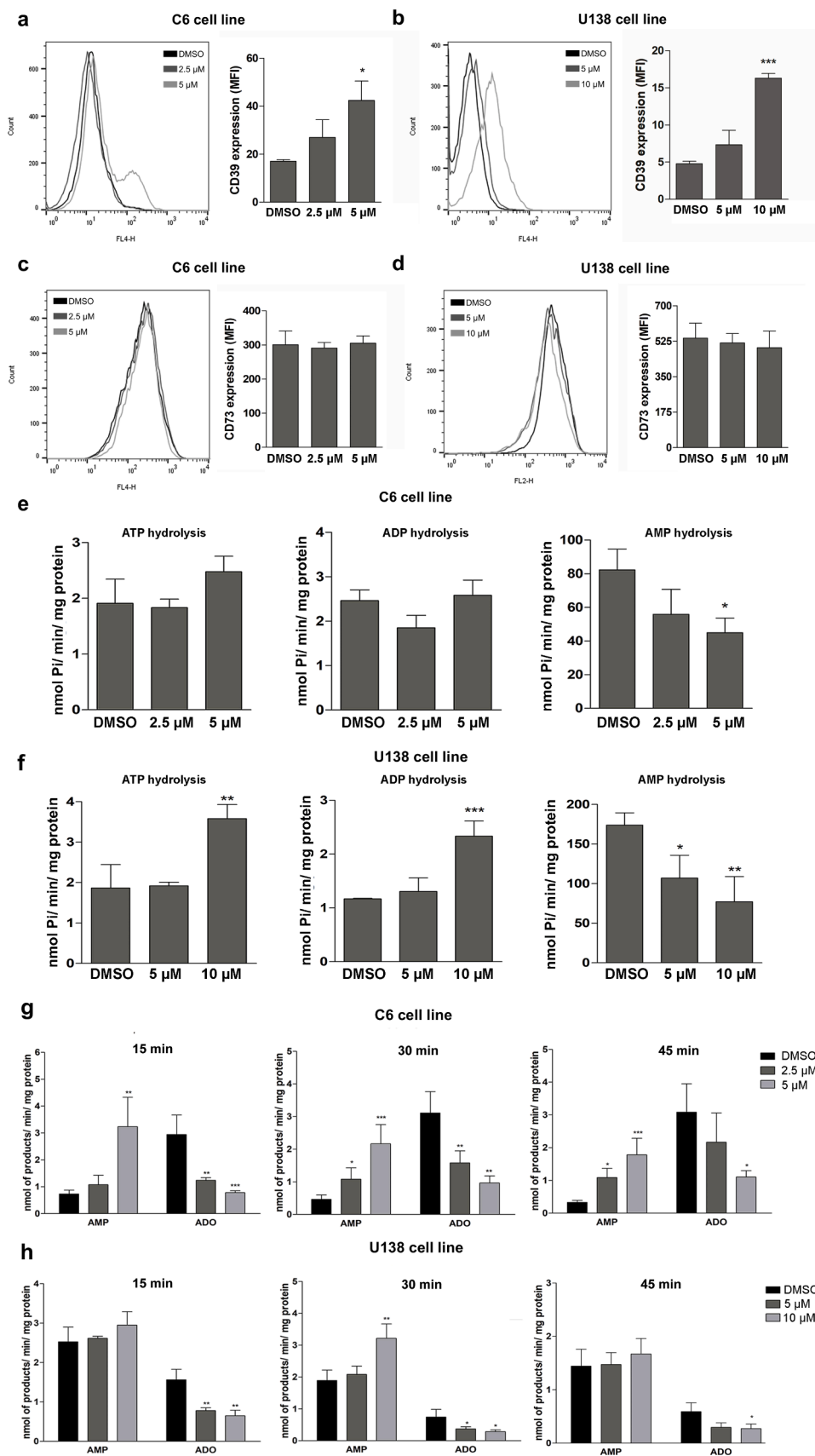
Fig. 4. BZP increased the CD39 expression, ATP and ADP hydrolysis, while decreased AMP hydrolysis and ADO formation without change of the CD73 expression. GBM cells were treated with BZP (2.5 μM/5 μM for C6 cell lines and 5 μM/10 μM for U138 cell lines) for 24 h. (a) Histogram and quantitative analysis of CD39 expression in C6 cells. (b) Histogram and quantitative analysis of CD39 expression in U138 cells. (c) Histogram and quantitative analysis of the CD73 expression in C6 cells. (d) Histogram and quantitative analysis of CD73 expression in U138 cells. (e) ATP, ADP and AMP hydrolysis in C6 cells. (f) ATP, ADP and AMP hydrolysis in U138. (g) Quantitative analysis of the ATP metabolism at times 15-, 30- and 45-min by HPLC in C6 cells. (h) Quantitative analysis of the ATP metabolism at times 15-, 30- and 45-min by HPLC in U138 cells. Data are presented as mean ± S.D. of three independent experiments. (*p<0.05 **p<0.01 *** p<0.001).
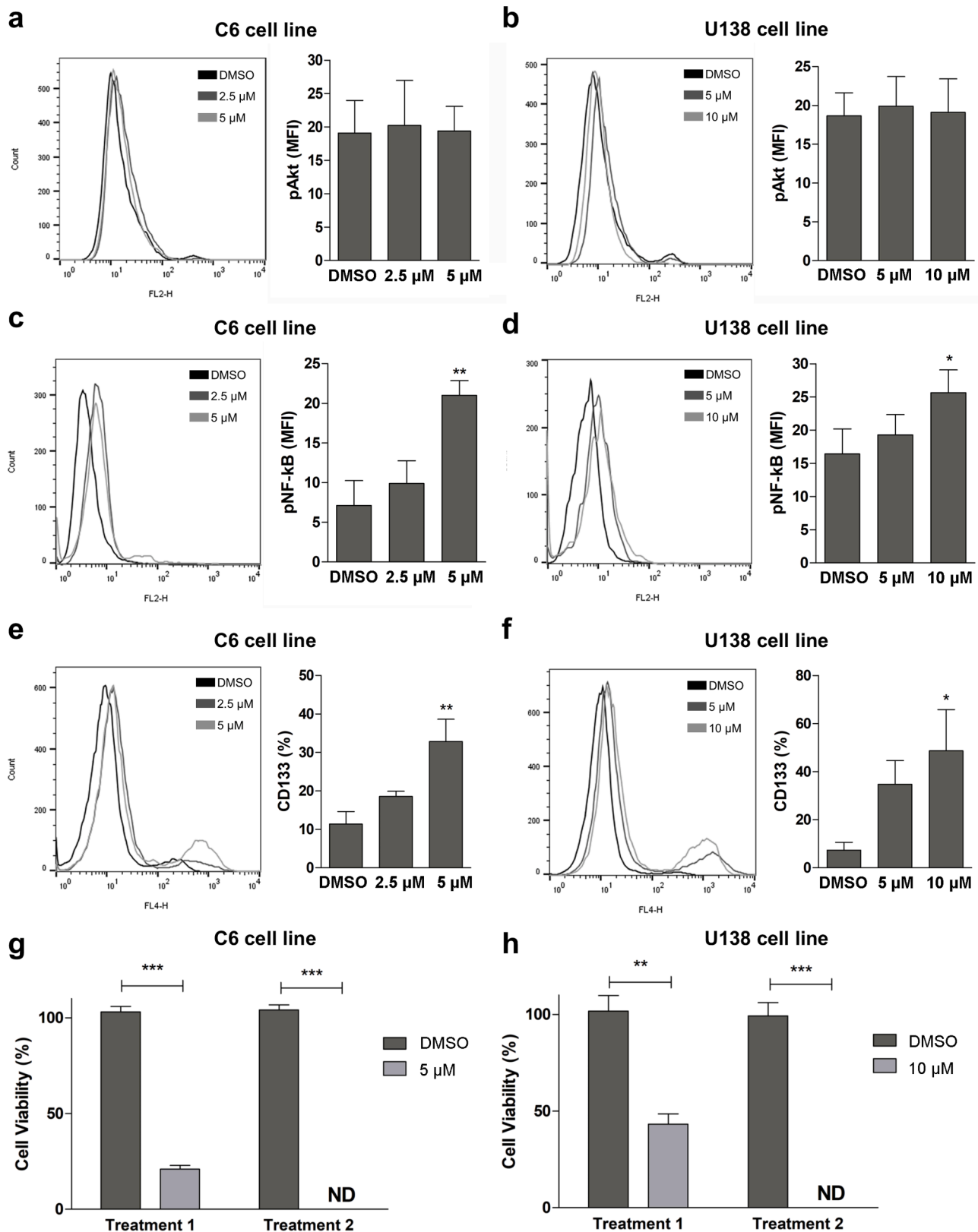
Fig. 5. BZP increased pNF-kB, without change of the Akt pathways and, keeps CD133⁺ cells, but two treatment cycles totally eliminate these cells. GBM cells were treated with BZP (2.5 μM/5 μM for C6 cell lines and 5 μM/10 μM for U138 cell lines) for 24 h. (a) Histogram and quantitative pAkt analysis to C6 cells. (b) Histogram and quantitative pAkt analysis to U138 cells. (c) Histogram and quantitative pNF-kB analysis to C6 cells. (d) Histogram and quantitative pNF-kB analysis to U138 cells. (e) Histogram and quantitative CD133 analysis in C6 cells. (f) Histogram and quantitative CD133 analysis in U138 cells. (g) Cell viability analysis in C6 cells (% of cells). (h) Cell viability analysis in U138 cells (% of cells). Data are presented as mean ± S.D. of three independent experiments. (*p<0.05 **p<0.01 ***p<0.001). ND: not detected

(Holmberg et al., 2014; Brugnoli et al., 2019). In addition, cancerous cells that have CD133$^+$ show greater chemoresistance (Soeda et al., 2009; Kim et al., 2017). As shown in Fig. 5e-f, treatment with BZP for 24h significantly increased the percentage of CD133$^+$ cells, from 11% in DMSO to 33% in BZP 5 μM (p = 0.0013, C6 cells) and, from 7% in DMSO to 49% in BZP 10 μM (p = 0.0112, U138 cells) (Figs. 5e and 5f) indicating these cells are more resistant to BZP treatment. Next, we decided to treat cells with different treatment cycles, quite common in chemotherapy, to analyze cellular resistance. Only two cycles at 5 μM and 10 μM for C6 and U138, respectively, were necessary to completely eliminate all cells, including resistant CD133$^+$ / NF-kB activated cells (Figs. 5g and 5h). This finding is very interesting since it has already been demonstrated that BZP is able to act selectively on resistant cells, mainly in CSCs (Ramírez et al., 2014).

4. Conclusions

Currently, many studies are focused on pathways related to cancer stem cell selection and drug resistance, among them NF-κB, CD73-ADO formation and CD133. In summary, we have demonstrated here that BZP treatment was able to reduce GBM growth by apoptosis and autophagy induction, without any change in Akt activation or interference on cell cycle progression. In addition, BZP was able to modulate the ectonucleotidases, increasing the expression and activity of CD39 enzyme, while it was able to inhibit the AMPase activity, with reduction of adenosine formation, without any change in CD73 expression, demonstrating a possible direct inhibition of this enzyme and corroborating the data obtained *in silico*. Curiously, we showed that one cycle of treatment with BZP increases the percentage of CD133$^+$ and the extent of activated NF-κB cells. Nevertheless, two cycles of BZP treatment managed to eliminate all cells, even NF-κB / CD133$^+$ cells. Finally, further research is needed to better understand the action of BZP in chemotherapy-resistant cancer cells.

Author statement

Amanda F. Dias: Conceptualization, Methodology, Investigation, Writing-Original draft preparation. **Juliete N. Scholl** and **Cesar E. J. Moritz**: Investigation, Data curation. **Luciano P. Kagami** and **Gustavo M. das Neves:** *in sílico* investigation. **Vera L. Eifler-Lima:** Supervision. **Olga Cruz-López, Ana Conejo-García and Jean Sévigny:** Investigation. **Ana M. O. Battastini** and **Joaquin María Campos:** Supervision, Funding acquisition. **Fabrício Figueiró:** Conceptualization, Supervision, Writing-Reviewing and Editing, Funding acquisition. All authors read and approved the final manuscript.

Declaration of Competing Interest

The authors declare that they have no conflict of interest.

Acknowledgments

References

Adamiak, M, Bujko, K, Brzezniakiewicz-Janus, K, Kucia, M, Ratajczak, J, Ratajczak, MZ, 2019. The inhibition of CD39 and CD73 cell surface ectonucleotidases by small molecular inhibitors enhances the mobilization of bone marrow residing stem cells by decreasing the extracellular level of adenosine. Stem Cell Rev Rep 15 (6), 892–899. https://doi.org/10.1007/s12015-019-09918-y.

Allard, D, Chrobak, P, Allard, B, Messaoudi, N, Stagg, J, 2019. Targeting the CD73-adenosine axis in immuno-oncology. Immunol Lett 205, 31–39. https://doi.org/10.1016/j.imlet.2018.05.001.

Andrade, P, de Fraga Dias, A, Figueiró, F, Torres, FC, Kawano, DF, Battastini, AMO, Carvalho, I, Silva, CHTP, Campos, JM, 2020. 1,2,3-Triazole tethered 2-mercaptobenzimidazole derivatives: design, synthesis and molecular assessment toward C6 glioma cell line. Future Med Chem 12 (8), 689–708. https://doi.org/10.4155/fmc-2019-0227.

Antonioli, L, Novitskiy, SV, Sachsenmeier, KF, Fornai, M, Blandizzi, C, Haskó, G, 2017. Switching off CD73: a way to boost the activity of conventional and targeted antineoplastic therapies. Drug Discov Today 22 (11), 1686–1696. https://doi.org/10.1016/j.drudis.2017.06.005.

Azambuja, JH, Schuh, RS, Michels, LR, Gelsleichter, NE, Beckenkamp, LR, Lenz, GS, de Oliveira, FH, Wink, MR, Stefani, MA, Battastini, AMO, Teixeira, HF, Braganhol, E, 2020. CD73 as a target to improve temozolomide chemotherapy effect in glioblastoma preclinical model. Cancer Chemother Pharmacol 85 (6), 1177–1182. https://doi.org/10.1007/s00280-020-04077-1.

Bai, D, Ueno, L, Vogt, PK, 2009. Akt-mediated regulation of NFκB and the essentialness of NFκB for the oncogenicity of PI3K and Akt. Int J Cancer 125 (12), 2863–2870. https://doi.org/10.1002/ijc.24748.

Barnholtz-Sloan, JS, Ostrom, Q, Cote, D, 2018. Epidemiology of Brain Tumors. Neurol Clin; 36 (3), 395–419. https://doi.org/10.1016/j.ncl.2018.04.001.

Bézivin, C, Tomasi, F, Lohézic-Le, D, Boustie, J, 2003. Cytotoxic activity of some lichen extracts on murine and human cancer cell lines. Phytomedicine; 10 (6-7), 499–503. https://doi.org/10.1078/094471103322331458.

Braganhol, E, Zamin, LL, Canedo, AD, Horn, F, Tamajusuku, ASK, Wink, MR, Salbego, C, Battastini, AMO, 2006. Antiproliferative effect of quercetin in the human U138MG glioma cell line. Anticancer Drugs; 17 (6), 663–671. https://10.1097/01.cad.0000215063.23932.02.

Braganhol, E, Tamajusuku, AS, Bernardi, A, Wink, MR, Battastini, AM, 2007. Ecto-5'-nucleotidase/CD73 inhibition by quercetin in the human U138MG glioma cell line. Biochim Biophys Acta 1770 (9), 1352–1359. https://doi.org/10.1016/j.bbagen.2007.06.003.

Braganhol, E, Morrone, FB, Bernardi, A, Huppes, D, Meurer, L, Edelweiss, MI, Lenz, G, Wink, MR, Robson, SC, Battastini, AM, 2009. Selective NTPDase2 expression modulates in vivo rat glioma growth. Cancer Sci 100 (8), 1434–1442. https://doi.org/10.1111/j.13497006.2009.01219.x.

Bradford, MM, 1976. A rapid and sensitive method for the quantitation of microgram quantities of protein utilizing the principle of protein-dye binding. Anal Biochem; 72, 248–254. https://doi.org/10.1006/abio.1976.9999.

Brugnoli, F, Grassilli, S, Al-Qassab, Y, Capitani, S, Bertagnolo, V, 2019. CD133 in breast cancer cells: more than a stem cell marker. J Oncol, 7512632. https://doi.org/10.1155/2019/7512632, 2019.

Burnstock, G, Knight, GE, 2004. Cellular distribution and functions of P2 receptor subtypes in different systems. Rev Cytol Clin 240, 231–304. https://doi.org/10.1016/S00747696(04)40002-3.

Cappellari, AR, Vasques, GJ, Bavaresco, L, Braganhol, E, Battastini, AM, 2012. Involvement of ecto-5'-nucleotidase/CD73 in U138MG glioma cell adhesion. Mol Cell Biochem 359 (1-2), 315–322. https://doi.org/10.1007/s11010-011-1025-9.

Ceruti, S, Abbracchio, MP, 2020. Adenosine Signaling in Glioma Cells. Adv Exp Med Biol 1202, 13–33. https://doi.org/10.1007/978-3-030-30651-9_2.

Chan, KM, Delfert, D, Junger, KD, 1986. A direct colorimetric assay for Ca2+-stimulated ATPase activity. Anal Biochem 157 (2), 375–380. https://doi.org/10.1016/00032697(86)906.40-8.

Chothiphirat, A, Nittayaboon, K, Kanokwiroon, K, Srisawat, T, Navakanitworakul, R, 2019. Anticancer Potential of Fruit Extracts from Vatica diospyroides Symington Type SS and Their Effect on Program Cell Death of Cervical Cancer Cell Lines. Sci. World J. 1–9. https://doi.org/10.1155/2019/5491904.

Ewing, TJ, Makino, S, Skillman, AG, Kuntz, ID, 2001. DOCK 4.0: search strategies for automated molecular docking of flexible molecule databases. Journal of computer-aided molecular design; 15 (5), 411–428. https://doi.org/10.1023/A:1011115820450.

Ferrin, TE, Huang, CC, Jarvis, LE, Langridge, R, 1988. The MIDAS display system. Journal of molecular graphics; 6 (1), 13–27. https://doi.org/10.1016/0263-7855(88)80054-7.

Figueiró, F, Mendes, FB, Corbelini, PF, Janarelli, F, Jandrey, EH, Russowsky, D, Eifler-Lima, VL, Battastini, AMO, 2014. A monastrol-derived compound, LaSOM 63, inhibits ecto-5'nucleotidase/CD73 activity and induces apoptotic cell death of glioma cell lines. Anticancer Res 34 (4), 1837–1842. Retrieved fromhttp://ar.iiarjournals.org/content/34/4/1837. long.

Figueiró, F, Oliveira, CP, Bergamin, LS, Rockenbach, L, Mendes, FB, Jandrey, EHF, Moritz, CEJ, Pettenuzzo, LF, Sévigny, J, Guterres, SS, Pohlmann, AR, Battastini, AMO, 2016. Methotrexate up-regulates ecto-5'-nucleotidase/CD73 and reduces the frequency of T lymphocytes in the glioblastoma microenvironment. Purinergic Signal 12 (2), 303–312. https://doi.org/10.1007/s11302-016-9505-8.

Geraghty, NJ, Watson, D, Sluyter, R, 2019. Pharmacological blockade of the CD39/CD73 pathway but not adenosine receptors augments disease in a humanized mouse model of graft-versus-host disease. Immunol Cell Biol 97 (6), 597–610. https://doi.org/10.1111/imcb.12251.

Herbener, VJ, Burster, T, Goreth, A, Pruss, M, von Bandemer, H, Baisch, T, Fitzel, R, Siegelin, MD, Karpel-Massler, G, Debatin, KM, Westhoff, MA, Strobel1, H, 2020. Considering the Experimental Use of Temozolomide in Glioblastoma Research. Biomedicines 8 (6), 151. https://doi.org/10.3390/biomedicines8060151.

Holmberg Olausson, K, Maire, CL, Haidar, S, Ling, J, Learner, E, Nister, H, Ligon, KL, 2014. Prominin-1 (CD133) defines both stem and non-stem cell populations in CNS development and gliomas. PLoS One 9 (9), e106694. https://doi.org/10.1371/journal.pone.0106694.

Kaltschmidt, C, Banz-Jansen, C, Benhidjeb, T, Beshay, M, Förster, C, Greiner, J, Hamelmann, E, Jorch, N, Mertzlufft, F, Pfitzenmaier, J, Simon, M, Schulte am Esch, J, Vordemvenne, T, Wähnert, D, Weissinger, F, Wilkens, L, Kaltschmidt, B, 2019. A role for NF-κB in organ specific cancer and cancer stem cells. Cancers (Basel) 11 (5), 655. https://doi.org/10.3390/cancers11050655.

Kim, EJ, Choi, CH, Park, JY, Kang, SK, Kim, YK, 2008. Underlying mechanism of quercetin-induced cell death in human glioma cells. Neurochem Res 33 (6), 971–979. https://doi.org/10.1007/s11064-007-9416-8.

Kim, YS, Kaidina, AM, Chiang, JH, Yarygin, KN, Lupatov, AY, 2017. Cancer stem cell molecular markers verified in vivo. Biochem. Moscow Suppl. Ser. B. 11 (1), 43–54. https://doi.org/10.1134/S1990750817010036.

Klionsky DJ, Abdalla FC, Abeliovich H, Abraham RT, Acevedo-Arozena A, Adeli K, Agholme L, Agnello M, Agostinis P, Aguirre-Ghiso JA, Ahn HJ, et al, 2016. Guidelines for the use and interpretation of assays for monitoring autophagy (3rd edition). Autophagy; 12(1): 1-222. https://doi.org/10.1080/15548627.2015.1100356.

Kocaturk, NM, Akkoc, Y, Kig, C, Bayraktar, O, Gozuacik, D, Kutlu, O, 2019. Autophagy as a molecular target for cancer treatment. Eur J Pharm Sci 134, 116–137. https://doi.org/10.1016/j.ejps.2019.04.011.

Kuntz, ID, Blaney, JM, Oatley, SJ, Langridge, R, Ferrin, TE, 1982. A geometric approach to macromolecule-ligand interactions. J Mol Biol 161 (2), 269–288. https://doi.org/10.1016/0022-2836(82)90153-x.

Ledur, PF, Villodre, ES, Paulus, R, Cruz, LA, Flores, DG, Lenz, G, 2012. Extracellular ATP reduces tumor sphere growth and cancer stem cell population in glioblastoma cells. Purinergic Signal; 8 (1), 39–48. https://doi.org/10.1007/s11302-011-9252-9.

Lee, SY, 2016. Temozolomide resistance in glioblastoma multiforme. Genes Dis 3 (3), 198–210. https://doi.org/10.1016/j.gendis.2016.04.007.

Lee, TG, Kim, SY, Kim, HR, Kim, H, Kim, CH, 2020. Radiation induces autophagy via histone H4 lysine 20 trimethylation in non-small cell lung cancer cells. Anticancer Rese 40 (5), 2537–2548. https://doi.org/10.21873/anticanres.14224.

Levy, JMM, Towers, CG, Thorburn, A, 2017. Targeting autophagy in cancer. Nat Rev Cancer 17 (9), 528–542. https://doi.org/10.1038/nrc.2017.53.

Li, M, Liang, RF, Wang, X, Mao, Q, Liu, YH, 2017. BKM120 sensitizes C6 glioma cells to temozolomide via suppression of the PI3K/Akt/NF-κB/MGMT signaling pathway. Oncol Lett 14 (6), 6597–6603. https://doi.org/10.3892/ol.2017.7034.

Liu, G, Pei, F, Yang, F, Li, L, Amin, AD, Liu, S, Buchan, JR, Cho, WC, 2017. Role of autophagy and apoptosis in non-small-cell lung cancer. Int J Mol Sci 18 (2), 367. https://doi.org/10.3390/ijms18020367.

Marchal, JA, Carrasco, E, Ramirez, A, Jiménez, G, Olmedo, C, Peran, M, Agil, A, Conejo-García, A, Cruz-López, O, Campos, JM, García, MÁ, 2013. Bozepinib, a novel small antitumor agent, induces PKR-mediated apoptosis and synergizes with IFNα triggering apoptosis, autophagy and senescence. Drug Des Devel Ther; 7, 1301–1313. https://doi.org/10.2147/DDDT.S51354.

Meng, EC, Shoichet, BK, Kuntz, ID, 1992. Automated docking with grid-based energy evaluation. J. Comput. Chem. 13 (4), 505–524. https://doi.org/10.1002/jcc.540130412.

Mizushima, N, Yoshimori, T, Levine, B, 2010. Methods in mammalian autophagy research. Cell 140 (3), 313–326. https://doi.org/10.1016/j.cell.2010.01.028.

Mutter, N, Stupp, R, 2006. Temozolomide: A milestone in neuro-oncology and beyond? Expert Rev. Anti-infect. Ther. 6 (8), 1187–1204. https://doi.org/10.1586/14737140.6.8.1187.

Neudert, G, Klebe, G, 2011. fconv: Format conversion, manipulation and feature computation of molecular data. Bioinformatics 27 (7), 1021–1022. https://doi.org/10.1093/bioinformatics/btr055.

Onorati, A, Dyczynski, M, Ojha, R, Amaravadi, RK, 2018. Targeting autophagy in cancer. Cancer 124 (16), 3307–3318. https://doi.org/10.1002/cncr.31335.

Ostrom, QT, Cioffi, G, Gittleman, H, Patil, N, Waite, K, Kruchko, C, Barnholtz-Sloan, JS, 2019. CBTRUS statistical report: primary brain and other central nervous system tumors diagnosed in the United States in 2012–2016. Neuro Oncol; 21 (S5), v1–v100. https://doi.org/10.1093/neuonc/noz150.

Peña-Morán, OA, Villarreal, ML, Álvarez-Berber, L, Meneses-Acosta, A, Rodríguez-López, V, 2016. Cytotoxicity, Post-Treatment Recovery, and Selectivity Analysis of Naturally Occurring Podophyllotoxins from Bursera fagaroides var. fagaroides on Breast Cancer Cell Lines. Molecules 21 (8), 1013. https://doi.org/10.3390/molecules21081013.

Pistritto, G, Trisciuoglio, D, Ceci, C, Garufi, A, D'Orazi, G, 2016. Apoptosis as anticancer mechanism: function and dysfunction of its modulators and targeted therapeutic strategies. Aging (Albany NY) 8 (4), 603–619. https://doi.org/10.18632/aging.100934.

Poillet-Perez, L, White, E, 2019. Role of tumor and host autophagy in cancer metabolism. Genes Dev 33 (11-12), 610–619. https://doi.org/10.1101/gad.325514.119.

Quispe, A, Zavala, C, Rojas, J, Posso, M, Vaisberg, A, 2006. Efecto citotóxico selectivo in vitro de murcin H (acetogenina de Annona muricata) en cultivos celulares de cáncer de pulmón. Rev. peru. med. exp. salud publica; 23 (4), 265–269. https://doi.org/10.17843/rpmesp.2006.234.1058.

Ramírez, A, Boulaiz, H, Morata-Tarifa, C, Perán, M, Jiménez, G, Picon-Ruiz, M, Agil, A, Cruz-López, O, Conejo-García, A, Campos, JM, Sánchez, A, García, MA, Marchal, JÁ, 2014. HER2-signaling pathway, JNK and ERKs Kinases, and cáncer stem-like cells

are targets of Bozepinib. Oncotarget; 5 (11), 3590–3606. https://doi.org/10.18632/oncotarget.1962.

Ramírez, D, Caballero, J, 2018. Is It Reliable to Take the Molecular Docking Top Scoring Position as the Best Solution without Considering Available Structural Data? Molecules 23 (5), 1038. https://doi.org/10.3390/molecules23051038.

Rinkenbaugh, AL, Cogswell, PC, Calamini, B, Dunn, DE, Persson, AI, Weiss, WA, Lo, DC, Baldwin, AS, 2016. IKK/NF-κB signaling contributes to glioblastoma stem cell maintenance. Oncotarget 7 (43), 69173–69187. https://doi.org/10.18632/oncotarget.12507.

Robson, SC, Sévigny, J, Zimmermann, H, 2006. The E-NTPDase family of ectonucleotidases: Structure function relationships and pathophysiological significance. Purinergic Signal; 2 (2), 409–430. https://doi.org/10.1007/s11302-006-9003-5.

Rockenbach, L, Bavaresco, L, Fernandes Farias, P, Cappellari, AR, Barrios, CH, Bueno Morrone, F, Oliveira Battastini, AM, 2013. Alterations in the extracellular catabolism of nucleotides are involved in the antiproliferative effect of quercetin in human bladder cancer T24 cells. Urol Oncol 31 (7), 1204–1211. https://doi.org/10.1016/j.urolonc.2011.10.009.

Russo, M, Russo, GL, 2018. Autophagy inducers in cancer. Biochem Pharmacol 153, 51–61. https://doi.org/10.1016/j.bcp.2018.02.007.

Ryu, CH, Yoon, WS, Park, KY, Kim, SM, Lim, JY, Woo, JS, Jeong, CH, Hou, Y, Jeun, SS, 2012. Valproic acid downregulates the expression of MGMT and sensitizes temozolomide-resistant glioma cells. J Biomed Biotechnol, 987495. https://doi.org/10.1155/2012/987495, 2012.

Shoichet, BK, Kuntz, ID, Bodian, DL, 1992. Molecular docking using shape descriptors. J. Comput. Chem. 13 (3), 380–397. https://doi.org/10.1002/jcc.540130311.

Soeda, A, Park, M, Lee, D, Mintz, A, Androutsellis-Theotokis, A, McKay, RD, Engh, J, Iwama, T, Kunisada, T, Kassam, AB, Pollack, IF, Park, DM, 2009. Hypoxia promotes expansion of the CD133-positive glioma stem cells through activation of HIF-1alpha. Oncogene; 28 (45), 3949–3959. https://doi.org/10.1038/onc.2009.252.

Stupp, R, Mason, WP, van den Bent, MJ, Weller, M, Fisher, B, Taphoorn, MJ, Belanger, K, Brandes, AA, Marosi, C, Bogdahn, U, Curschmann, J, Janzer, RC, Ludwin, SK, Gorlia, T, Allgeier, A, Lacombe, D, Cairncross, JG, Eisenhauer, E, Mirimanoff, RO, 2005. Radiotherapy plus concomitant and adjuvant temozolomide for glioblastoma. N Engl J Med 352 (10), 987–996. https://doi.org/10.1056/NEJMoa043330.

Tavana, E, Mollazadeh, H, Mohtashami, E, Modaresi, SMS, Hosseini, A, Sabri, H, Soltani, A, Javid, H, Afshari, AR, Sahebkar, A, 2020. Quercetin: A promising phytochemical for the treatment of glioblastoma multiforme. BioFactors; 46 (3), 356–366. https://doi.org/10.1002/biof.1605.

Towner, RA, Smith, N, Saunders, D, Brown, CA, Cai, X, Ziegler, J, Mallory, S, Dozmorov, MG, De Souza, PC, Wiley, G, Kim, K, Kang, S, Kong, DS, Kim, YT, Fung, KM, Wren, JD, Battiste, J, 2019. OKN-007 Increases temozolomide (TMZ) sensitivity and suppresses TMZ-resistant glioblastoma (GBM) tumor growth. Transl Oncol 12 (2), 320–335. https://doi.org/10.1016/j.tranon.2018.10.002.

Uribe, D, Torres, Á, Rocha, JD, Niechi, I, Oyarzún, C, Sobrevia, L, San Martín, R, Quezada, C, 2017. Multidrug resistance in glioblastoma stem-like cells: Role of the hypoxic microenvironment and adenosine signaling. Mol Aspects Med 55, 140–151. https://doi.org/10.1016/j.mam.2017.01.009.

Voelter, W, Zech, K, Arnold, P, Ludwig, G, 1980. Determination of selected pyrimidines, purines and their metabolites in serum and urine by reversed-phase ion-pair chromatography. J Chromatogr; 199, 345–354. https://doi.org/10.1016/s00219673(01)91386x.

White, E, 2015. The role for autophagy in cancer. J Clin Invest 125 (1), 42–46. https://doi.org/10.1172/JCI73941.

White, E, Karp, C, Strohecker, AM, Guo, Y, Mathew, R, 2010. Role of autophagy in suppression of inflammation and cancer. Curr Opin Cell Biol 22 (2), 212–217. https://doi.org/10.1016/j.ceb.2009.12.008.

Wijaya, J, Fukuda, Y, Schuetz, JD, 2017. Obstacles to brain tumor therapy: key ABC transporters. Int J Mol Sci 18 (12), 2544. https://doi.org/10.3390/ijms18122544.

Wink, MR, Lenz, G, Braganhol, E, Tamajusuku, AS, Schwartsmann, G, Sarkis, JJ, Battastini, AM, 2003. Altered extracellular ATP, ADP and AMP catabolism in glioma cell lines. Cancer Lett; 198 (2), 211–218. https://doi.org/10.1016/s0304-3835(03)00308-2.

Wong, RSY, 2011. Apoptosis in cancer: from pathogenesis to treatment. J Exp Clin Cancer Res 30 (1), 87. https://doi.org/10.1186/1756-9966-30-87.

Xu, S, Shao, QQ, Sun, JT, Yang, N, Xie, Q, Wang, DH, Huang, QB, Huang, B, Wang, XY, Li, XG, Qu, X, 2013. Synergy between the ectoenzymes CD39 and CD73 contributes to adenosinergic immunosuppression in human malignant gliomas. Neuro-Oncology; 15 (9), 1160–1172. https://doi.org/10.1093/neuonc/not067.

Xu, X, Lai, Y, Hua, ZC, 2019. Apoptosis and apoptotic body: disease message and therapeutic target potentials. Biosci Rep 8 (4), 603–619. https://doi.org/10.1042/BSR20180992.

Yamada, R, Nakano, I, 2012. Glioma stem cells: their role in chemoresistance. World Neurosurg; 77 (2), 237–240. https://doi.org/10.1016/j.wneu.2012.01.004.

Yan, G, Wang, Y, Chen, J, Zheng, W, Liu, C, Chen, S, Wang, L, Luo, J, Li, Z, 2020. Advances in drug development for targeted therapies for glioblastoma. Med Res Rev 40 (5), 1950–1972. https://doi.org/10.1002/med.21676.

Yang, KL, Khoo, BY, Ong, MT, Yoong, ICK, Sreeramanan, S, 2020. In vitro anti-breast cancer studies of LED red light therapy through autophagy. Breast Cancer. https://doi.org/10.1007/s12282-020-01128-6 [Epub-ahead of Print].

Zhou, LX, Lou, YN, Fu, SL, Ge, P, Zhuang, H, 2006. Effect of quercetin on proliferation of rat glioma C6 cells. J. Jilin Agric. Univ. (Med. Edn. 32 (2), 251–253. Retrieved from. http://xuebao.jlu.edu.cn/yxb/EN/abstract/abstract1585.shtml.

Zhu, P, Du, XL, Lu, G, Zhu, JJ, 2017. Survival benefit of glioblastoma patients after FDA approval of temozolomide concomitant with radiation and bevacizumab: A population-based study. Oncotarget; 8 (27), 44015–44031. https://doi.org/10.18632/oncotarget.17054.

Zimmermann, H, 2001. Ectonucleotidases: Some recent developments and a note on nomenclature. Drug Dev Res; 52 (1-2), 44–56. https://doi.org/10.1002/ddr.1097.